Pump−Probe Spectroscopy of the Hydrated Electron in Reverse Micelles

Young Jong Lee, Tak W. Kee, Tieqiao Zhang, and Paul F. Barbara*

Department of Chemistry and Biochemistry, University of Texas at Austin, Austin, Texas 78712

Received: November 3, 2003; In Final Form: January 12, 2004

Ultrafast spectroscopy was used to investigate the excited state dynamics and photochemistry of the hydrated electron in the water pool of a reverse micelle (RM) comprised of water and the surfactant, AOT, dissolved in an isooctane solution. Solvated electrons were generated in the isooctane solvent by photoionization (three photons of 400 nm). The isooctane-solvated electrons were observed to rapidly attach to the RM and relax in the water pool within 1 ps. A second 400 nm excitation pulse was employed to excite the equilibrated hydrated electron in the RM water pool, inducing an electron transfer reaction with the surfactant molecules. The ultrafast data as a function of RM size offer new insights on spatial confinement effects on the chemistry and relaxation dynamics of excess electrons in nanometer-sized water pools.

Introduction

The nanometer-sized water pool of a reverse micelle (RM) offers a unique environment to study the effect of spatial confinement on the energetics, chemical reactions, and relaxation processes of the hydrated electron. The spectroscopy of the hydrated electron, e_{aq}^-, in the interior of RMs has been extensively investigated by both experiment and theory.[1−5] RMs have a water pool surrounded by a surfactant layer and typically are comprised of a water/surfactant/nonpolar-solvent mixture, such as the well-known water/AOT/alkane system (where AOT is Aerosol OT). Solutions of well-structured RMs can be made reliably with a radius of the RM water pool, R_w, in the range of 10−90 Å.[6−11] For sufficiently large water pools ($R_w > 30$ Å), the absorption spectrum of e_{aq}^- is indistinguishable from its spectrum in bulk water, suggesting very little perturbation of e_{aq}^- by the surfactant layer.[3,12,13] However, for small water pools, the e_{aq}^- is perturbed by the surfactant headgroups and counterions resulting in a "blue shift" of the absorption spectrum of the hydrated electron.[2,3,12,13] Hydrated electrons in RMs have been prepared by attachment of alkane-solvated electrons (pulse radiolysis)[3,13−15] to RMs or by photoionization of aromatic electron donors, such as phenothiazine.[2,12] In both cases, lifetimes of the hydrated electron in the RM are on the order of 10^{-7} s as a result of the reaction with AOT.[2,3,13]

Ultrafast measurements on the relaxation dynamics and chemical reaction kinetics of excited states of the hydrated electron in the water pool of RMs are presented in the present paper and are compared to previously obtained analogous results for bulk water. In bulk water, the ground state of the hydrated electron is localized in a solvent cavity, is approximately spherical, and has a radius of ∼3 Å.[16] The lowest excited state of the hydrated electron corresponds to a p state, e_p^-, which has been prepared by optical excitation in the 600−1000 nm region.[17,18] The second excited state of the hydrated electron corresponds to a highly delocalized quasi conduction band, e_{CB}^-, with an extraordinarily large radius of >30 Å.[18,19] It has been prepared by excitation at <450 nm.[17,18] The e_p^- and e_{CB}^- states have short lifetimes, 300 and 50−100 fs, respectively,[20,21] because of rapid internal conversion. The close similarity of the spectroscopy of e_{aq}^- in the water pool of a RM to that in bulk water strongly suggests that the states in RM water pools are analogous to those for bulk water.

The electron transfer (ET) reactions of e_p^- and e_{CB}^- in bulk water with various electron acceptor (e.g., Cd^{2+}) solutes have also been extensively investigated.[19,22] This ultrafast ET reaction occurs by a "static scavenging" mechanism on a time scale too short to allow for spatial diffusion of the electron acceptors. The published ET rates are significantly larger for e_{CB}^- than for e_p^- due primarily to a size effect, that is, e_{CB}^- is in "contact" with a much larger number of electron acceptors because of its larger radius. However, on a per acceptor basis the ET rates for e_{CB}^- are actually smaller than those for e_p^-. This latter effect has been attributed to an electron density effect for which the ET rate per acceptor (in contact with e_p^- or e_{CB}^-) is proportional to the donor electron density and inversely proportional to the electron "volume" given by the cube of the effective electron radius.

In this work, ultrafast pump−probe spectroscopy is used to investigate the relaxation dynamics and ET reactions of a hydrated electron in the water pool of an AOT RM. The results are consistent with an ET reaction of e_{CB}^- with AOT, which forms the "wall" of the RM. The observed RM water pool size dependencies of the yield of the ET reaction and the relaxation dynamics are extensively explored herein. The yield of the ET reaction and the relaxation rate are observed to decrease with increasing size of the RMs. These trends indicate that spatial confinement of e_{CB}^- can play an important role in the ET reaction rates and dynamics of photoexcited hydrated electrons in RM water pools.

Experimental Section

The femtosecond laser system for the 3-pulse transient absorption spectroscopy has been described earlier.[19,22] Briefly, a multipass amplified Ti:sapphire system produced 35 fs pulses, centered at 800 nm, at a 1 kHz repetition rate. The laser beam was divided into three beams. The first beam was doubled to 400 nm to photoionize isooctane, and the second was either doubled for 400 nm pulses or untouched for 800 nm pulses,

* Author to whom correspondence should be addressed. E-mail: p.barbara@mail.utexas.edu.

10.1021/jp0373393 CCC: $27.50
Published on Web 02/20/2004

which pumped hydrated electrons in the RM. Pulse energies of the ionization and pump beams were kept at 20 and 2 μJ/pulse, respectively. The third beam generated white light continuum and was compressed by a prism pair. The 650 nm portion of the continuum was preselected before the sample and used as a probe. The instrument responses (fwhm) of 60 and 80 fs were used for fitting 2- and 3-pulse data, respectively. All quantitative measurements in this paper used a pump energy of 2 μJ/pulse ($\sim$0.03 J/cm^2), for which the initial excited state population fraction is below 20% and multiphoton absorption by e_{aq}^- can be neglected.

AOT (Aerosol OT, sodium bis(2-ethylhexyl)sulfosuccinate, Aldrich), AIB (Aerosol IB, sodium bis(2-methylpropyl)sulfosuccinate, Fluka), and isooctane (Aldrich) were purchased and used without any further purification. SDSS (sodium dimethyl sulfosuccinate) was synthesized with dimethylmaleate and sodium bisulfite,[23] and after recrystallization and vacuum-drying, a purity of >99.7% was confirmed with NMR. The molar ratio of water to the surfactant, that is, $W = [H_2O]/[AOT]$, was varied from 7 to 50, and AOT concentrations were kept at 0.3 M. These solutions are all in the reverse micellar phase in the phase diagram of H_2O/AOT/isooctane.[24] The reported thresholds of conductivity percolation and the phase transition boundary of the H_2O/AOT/isooctane system[25] are far above the experimental concentrations used in this paper, ensuring isolated RMs. All measurements were made with freshly made water/AOT/isooctane solutions to avoid buildup of reaction products and change of composition by evaporation of solvents. Solutions were flowed using a gravity-driven wire-guided jet nozzle[26] with a thickness of 80 $\pm$ 20 μm. The sample temperature was maintained at 23 °C for the experiments.

Results and Discussion

Electron Attachment of Solvated Electrons in Isooctane to a Reverse Micelle. In this work, electron/hole pairs in isooctane (IP = 8.4 eV)[27] were generated by 3-photon ionization (400 nm, 9.3 eV). In neat isooctane, geminate recombination was observed to occur with a decay constant of 400 fs (see Figure 1a). In the presence of a RM, however, some of the electrons generated in isooctane attach to the RM and become hydrated in the RM water pools. For example, consider the transient data in Figure 1a for the RM solutions with the molar ratios $W = 20$ and 50. The early decrease in optical density (OD) for these solutions is due to geminate recombination of electron/hole pairs in isooctane, while the subsequent increase in OD is assigned to the appearance of the hydrated electron, e_{aq}^-, in the RM.

For RM solutions at constant [AOT] = 0.3 M, the attachment yield is observed to increase as W is increased because of more effective scavenging by a larger RM.[14,15,28] For $W = 50$, the rising component due to the hydrated electron in the water pool actually exceeds at its peak the initial OD of photogenerated electrons in the isooctane. This indicates that the hydrated electron has a higher absorption coefficient at 650 nm than the electron/hole pairs in isooctane at the same wavelength and demonstrates that at long times the transient OD data is due predominantly to the transition ($e_{aq}^- \rightarrow e_p^-$) of the hydrated electron in the RM water pool.[28] The constant OD of the hydrated electrons at times up to 120 ps (Figure 1b) is consistent with previously reported e_{aq}^- lifetimes of hundreds of nanoseconds in AOT RMs.[2,3,13]

Pump−Probe Spectroscopy of a Hydrated Electron in the Water Pool of a Reverse Micelle. Ultrafast pump−probe data on e_{aq}^- in the water pool of a RM are shown in Figure 2. The

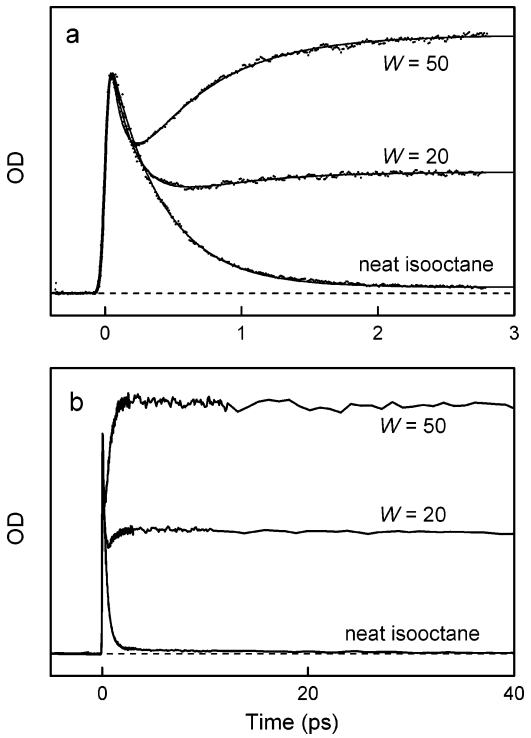

Figure 1. Comparison of transient absorption of neat isooctane and reverse micelles in isooctane ($W = 20$ and 50 and [AOT] = 0.3 M), with an ionization pulse of 400 nm and a probe pulse of 650 nm. The solid lines through the data are the multiexponential least-squares fit. The data of isooctane is well fitted with two exponentially decaying functions ($\tau_1 = 400$ fs, $A_1 = 0.97$ and $\tau_2 = 39$ ps, $A_2 = 0.03$). In the presence of reverse micelles, the data are fitted with three exponential functions: for $W = 20$, $\tau_1 = 160$ fs, $A_1 = 1.0$, $\tau_2 = 510$ fs, $A_2 = -0.3$, and $\tau_3 = 100$ ns, $A_3 = 0.33$; for $W = 50$, $\tau_1 = 100$ fs, $A_1 = 1.0$, $\tau_2 = 570$ fs, $A_2 = -0.84$, and $\tau_3 = 100$ ns, $A_3 = 1.1$. The second rising component ($A_2 < 0$) involves the dynamics of electron attachment and solvation in the water pools. The third slow time constants, τ_3, are adopted from the lifetime of e_{aq}^- in AOT reverse micelles.[2,3,13]

e_{aq}^- was excited by a pump pulse of either 400 or 800 nm, which was delayed 50 ps after the much more intense 400 nm photoionization pulse. The transient absorbance (ΔOD) in Figure 2 at 650 nm reveals evidence of both a relaxation to the ground state on the subpicosecond time scale and a long-term "bleach" due to a photoinduced reaction of the excited electron. The observed data are highly analogous and similar in kinetic form and time scales to the transient spectroscopy of e_{aq}^- in bulk water in the presence of a high concentration of electron acceptors.[19,22] For bulk solutions, the long-term "bleach" is due to an excited state ET reaction of the hydrated electron (see the Introduction). As in the case of bulk solutions, the transient data for the hydrated electrons in the water pools reveal a dependence of the photoinduced reaction yield on excitation wavelength. For 400 nm excitation, which by analogy to the bulk water prepares e_{CB}^-, the yield (Y_D) is 0.35 $\pm$ 0.02. In contrast, the yield is much smaller ($Y_D = 0.06 \pm 0.02$) for 800 nm excitation, which corresponds to e_p^- preparation. The present paper is focused on the more efficient e_{CB}^- reaction, that is, 400 nm excitation.

It should be noted that although the conduction band (e_{CB}^-) of the water pool is highly delocalized relative to the size of a solvated electron water cavity, it is still formally a particle-in-a-box state of the RM. Thus, the term "conduction band" for a RM in this paper refers to a particle-in-a-box-like state in the water pool of the RM.

We have considered two alternatives for the e_{CB}^- reaction: (i) an ET reaction of the e_{CB}^- with the surfactant AOT and (ii)

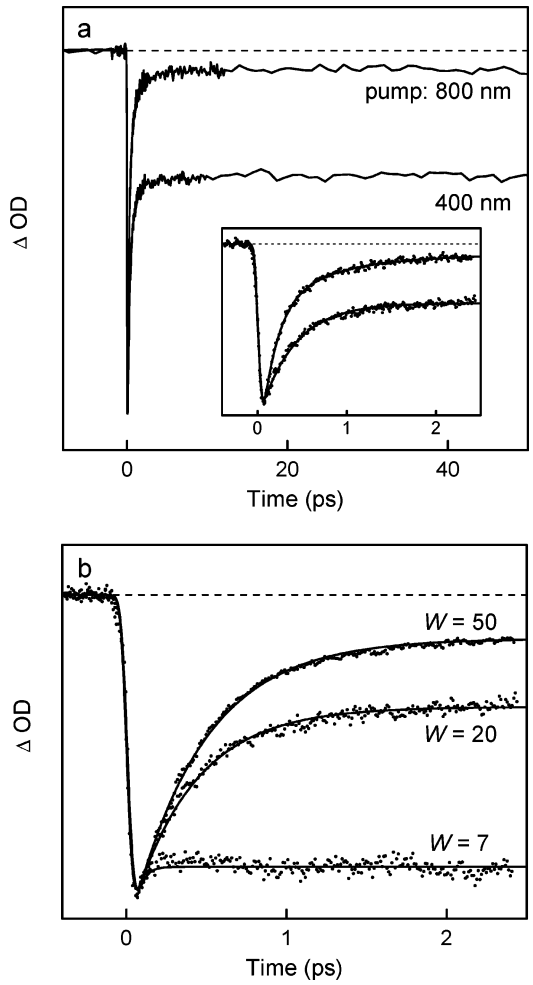

Figure 2. (a) Transient ΔOD (change in optical density) data of the hydrated electron (e_{aq}^-) in a reverse micelle ($W = 20$ and [AOT] = 0.3 M) with two different pumps of 400 and 800 nm and a probe of 650 nm. The pump pulse arrives 50 ps after the ionization pulse, when the solvation of the attached electron in the water pools has completely finished. The solid lines in the inset are the best fit of 400 and 800 nm pump transients. The data are well fit by a model function $\Delta OD(t) = \Sigma_i A_i \exp(-t/\tau_i) + C$, using, for the 400 nm pump, $A_1 = -0.65$, $\tau_1 =$ 400 fs, and $C = -0.35$ and, for the 800 nm pump, $A_1 = -0.64$, $\tau_1 =$ 160 fs, $A_2 = -0.30$, $\tau_2 = 700$ fs, and $C = -0.06$. The ΔOD data do not fully recover to zero, but show a clear photoinduced depletion of e_{aq}^-. (b) Time evolutions of the transient ΔOD data of differently sized reverse micelles ($W = 7$, 20, and 50) with a 400 nm pump and a 650 nm probe. For simplicity, the other data ($W = 12$ and 30) are not shown in the figure. The fitting parameters are listed in Table 1.

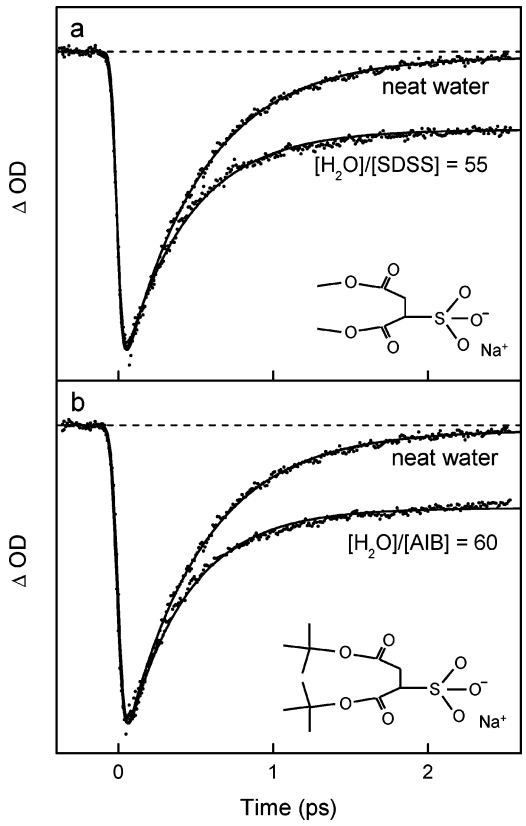

Figure 3. ΔOD data of the excited state (e_{CB}^-) prepared with a 400 nm pump in (a) SDSS and (b) AIB aqueous solutions, which are compared with the ΔOD data of neat water. The e_{aq}^- was excited by a 400 nm pulse delayed 50 ps after the 400 nm photoionization pulse. For the SDSS solution, the molar ratio $W = [H_2O]/[SDSS] = 55$; for the AIB solution, $W = [H_2O]/[AIB] = 60$. In neat water, e_{CB}^- is fully recovered with a decay constant of 500 fs, whereas in the presence of SDSS and AIB electron-transfer reactions cause the permanent depletion. For the SDSS solution, Y_D is 0.23, and for the AIB solution, Y_D is 0.24.

TABLE 1: Summary of the Values for the Electron Depletion of e_{CB}^- in Reverse Micelles

W	R_w (Å)[a]	Y_D	τ (fs)
7	10.5	0.75 ± 0.10[b]	42 ± 7[b]
12	18	0.51 ± 0.02	270 ± 15
20	30	0.35 ± 0.02	400 ± 15
30	45	0.19 ± 0.01	445 ± 15
50	75	0.13 ± 0.01	460 ± 16

[a] Values are calculated from R_w (Å) $= 1.5W$.[6–8] [b] The measured recovery time is too short for the time resolution to provide reliable values, and the presented errors are obtained from the standard deviations of multiple measurements.

a photo detachment (i.e., "escape") of the hydrated electron from the reverse micelle followed by recombination with the isooctane "hole" (also an ET reaction). To independently evaluate the e_{CB}^- reaction with AOT, we investigated the photoinduced reaction yields in non-RM environments containing AOT-like reactants, which have the same sulfosuccinate headgroup as AOT but shorter alkyl chains. In particular, non-RM aqueous solutions containing either sodium bis(2-methylpropyl)sulfosuccinate (AIB) or sodium dimethyl sulfosuccinate (SDSS) were investigated to mimic the "chemical environment" of AOT RM without the possibility of a photodetachment from the water pool of the RM. In Figure 3 the ΔOD data of the SDSS and AIB solutions show a permanent depletion in OD, with a photoinduced reaction yield that is similar to that of the AOT RM (Figure 2). By analogy, we assign the observed reaction of e_{CB}^- in the RM to a simple ET reaction of e_{CB}^- with AOT, rather than RM electron detachment. More detailed investigations, however, will be necessary to completely rule out the detachment as a competitive pathway, since preliminary results on a different RM system suggest that a detachment also can occur in some cases, albeit with a lower yield than the ET reaction of e_{CB}^- with AOT.[29] The actual products of the ET reaction are unknown but probably involve reduction of the AOT molecule followed by fragmentation of the radical anion.[4]

ET Rates as a Function of a Water Pool Radius. The data (Table 1, Figure 2) reveal a strong dependence of the e_{CB}^- ET yield on the radius of the RM water pool, R_w (which can be estimated from W).[6–8] As in the case of e_{CB}^- reactions in bulk solutions,[19] we assume the ET yield reflects a competition of the e_{CB}^- ET rate and the e_{CB}^- relaxation rate to the lower p and s states. Thus, the data in Table 1 indicate that both the ET yield (Y_D) and ET rates monotonically decrease with an

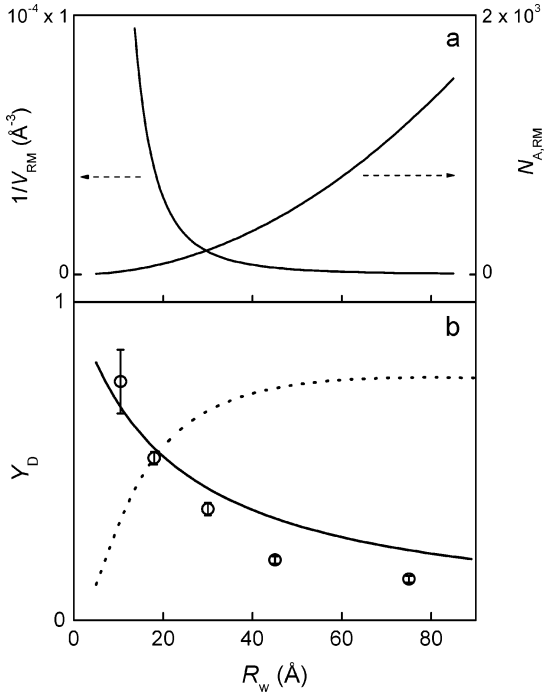

Figure 4. (a) $1/V_{RM}$, proportional to the electron density in the *confinement* effect on e_{CB}^- and the number of acceptors per reverse micelle ($N_{A,RM}$) using the molecular surface area of AOT $A_{A,m} = 60$ Å^2 molecule^{-1}.[7] (b) Comparisons of the Y_D measured using a 400 nm pump and a 650 nm probe and the Y_D calculated considering the *distance* effect and the *confinement* effect. The dotted line is from the *distance* model (eq 6) with a previously estimated size of e_{CB}^- of $\beta^{-1} = 30$ Å, and $\tau_{CB} = 75$ fs,[19] and with a fitted value of $k^0_{ET,A} = 3.8 \times 10^{11}$ s^{-1}. The solid line is calculated from the *confinement* model (eq 3) using the previously estimated values, $k^s_{ET,A} = 5 \times 10^{13}$ s^{-1}, $r_{e_{aq}^-} = 3$ Å, and $\tau_{CB} = 75$ fs.[19] The effect of the polydispersity of the size distribution of reverse micelles is checked with the Schulz distribution function[7] with the polydispersity (σ/R_w), and the simulation with a value of 0.2 for polydispersity[11] shows a negligible difference in Y_D (<3%) compared to the experimental error.

increasing water pool radius. A simple quantitative model for the RM ET reaction can be constructed using elements from our published treatment of ET between *hydrated electron states* and electron acceptors in bulk solution. The bulk solution model was based on the ET rates being proportional to two independent factors: (i) the electron density of the highly delocalized *hydrated electron state* at the position of the highly localized acceptor orbitals and (ii) the number of acceptor molecules located within the effective radius of the e_{CB}^-. The application of this model to the RM water pools leads to the following picture. Photoexcitation of the e_{aq}^- (~3 Å)[16] located randomly in the water pool induces the ET reaction by preparing a highly delocalized e_{CB}^- state (>30 Å)[18,19] that is electronically overlapped with the AOT acceptors at the RM edge.

The electron density effect and the number of acceptor group effect have an opposite size dependence for the water pool case. This is demonstrated qualitatively in Figure 4a and schematically in Figure 5. The *number of AOT acceptor molecules per reverse micelle* ($N_{A,RM}$) increases with R_w, since it is proportional to the surface area. In contrast, the effective electron density of e_{CB}^- at the acceptors at edge of the RM will tend to decrease with increasing R_w as a result of a distance effect and a confinement effect. The *distance* effect involves the distance between the "center" of e_{CB}^- and the location of the AOT groups, which should decrease with R_w. This should be an important factor in the rate when R_w is much larger than the radius of e_{CB}^- such that the e_{CB}^- state is too far from the AOT

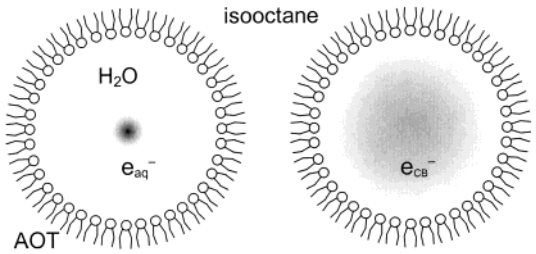

Figure 5. Schematic representation of e_{aq}^- and e_{CB}^- in reverse micelles.

groups to allow for good overlap. Second, for R_w values comparable to the radius of e_{CB}^-, one would expect a *confinement* effect in which the electron density of e_{CB}^- at AOT (and thus the ET rate) is inversely proportional to the volume of the RM water pool (see Figure 4a). On the basis of previous estimates of the radius of the e_{CB}^- state (>30 Å),[18,19] the confinement effect should be a factor for the R_w dependences investigated in Figure 2b.

A simple expression for the ET rate, k_{ET}, within the confinement model can be simply adopted from the Kee et al. treatment of hydrated electron ET reactions in bulk water.[19] In the Kee et al. model, the ET rate per acceptor, $k_{ET,A}(r_x)$, between any form of the hydrated electron and a "good" electron acceptor fits a "universal curve" as follows,

$$k_{ET,A}(r_x) = \frac{k^s_{ET,A}\, r^3_{e_{aq}^-}}{r_x^{\,3}} \qquad (1)$$

where r_x is the radius of the state in question. $k^s_{ET,A}$ is an experimentally determined constant assigned to the static ET rate constant for e_{aq}^- using only the previously determined mean values for NO_3^-, Cd^{2+}, and SeO_4^{2-} in aqueous solutions.[19] For the RM case, we need to simply identify r_x with R_w and take into account the number of AOT acceptors. The total ET rate (eq 2) is a product of $k_{ET,A}(R_w)$ and the number of acceptors in the RM, $N_{A,RM}(R_w) = 4\pi R_w^2/A_{A,m}$, where $A_{A,m}$ is the molecular surface area of the acceptor ($A_{A,m} = 60$ Å^2 molecule^{-1} for AOT).[7]

$$k_{ET}(R_w) = N_{A,RM}(R_w) k_{ET,A}(R_w) \qquad (2)$$

By use of previous estimates for the e_{CB}^- lifetime, τ_{CB}, and a simple expression for the yield, a prediction (eq 3) for the Y_D as a function of R_w is derived with no adjustable parameters.

$$Y_D(R_w) = \frac{k_{ET}(R_w)}{k_{ET}(R_w) + 1/\tau_{CB}} \qquad (3)$$

The agreement between eq 3 (solid line) and the experimental data is excellent (see Figure 4b). This implies that a spatial confinement effect may indeed be very important for the e_{CB}^- ET reaction in the water pool of RM.

We have also considered how the ET rate should vary without electron confinement effect on the e_{CB}^- state. For this calculation, the ET rate per electron acceptor was expressed in the usual way as[30]

$$k_{ET,A}(\mathbf{r}_e, \mathbf{R}_A) = k^0_{ET,A} \exp(-\beta|\mathbf{r}_e - \mathbf{R}_A|) \qquad (4)$$

where $\mathbf{r}_e$ and $\mathbf{R}_A$ are position vectors of an electron and an acceptor starting from the center of the RM, before a pump pulse arrives. β^{-1} was chosen to be 30 Å, the estimated radius

of the e_{CB}^- state.[19] The ET rate, $k_{ET}(r_e, R_w)$, of an electron at $r_e = |\mathbf{r}_e|$ is the sum of $k_{ET,A}$ for all acceptors, which can be expressed as an integral of $k_{ET,A}$ over the area element dA, since $|\mathbf{R}_A| = R_w$ is constant for all acceptors. Then,

$$k_{ET}(r_e,R_w) = \int k^0_{ET,A} \exp(-\beta|\mathbf{r}_e - \mathbf{R}_A|)\, dA \qquad (5)$$

and the yield of depletion due to the ET reaction of an electron located at r_e is

$$Y_D(r_e,R_w) = \frac{k_{ET}(r_e,R_w)}{k_{ET}(r_e,R_w) + 1/\tau_{CB}} \qquad (6)$$

The predicted ET yield from eq 6 actually increases with R_w (the dotted line in Figure 4b), which is opposite to experimental data.[31] This is apparently further evidence that spatial confinement of the e_{CB}^- is important in the ET reaction in the water pools of RMs.

Another form of evidence that the electrons in the water pool are sensitive to the RM environment is found in the observed dependence of the relaxation rates on the RM size (Table 1). The relaxation times reflect a combination of excited state and ground state relaxation. In large water pools, the observed values are close to those observed in bulk water, but in the smaller RM environments the acceleration in rate apparently reflects a significant interaction with the AOT surface.

Conclusion

Ultrafast pump−probe spectroscopy on the relaxation dynamics and ET reactions of a hydrated electron in a water pool is consistent with an ET reaction of the e_{CB}^- with the AOT, which forms the "wall" of the RM. The observed RM water pool size dependencies of the yield of the ET reaction and the relaxation dynamics were extensively explored. The yield of the ET reaction and the relaxation rate were observed to decrease with increasing size of the RMs suggesting that a significant spatial confinement effect on e_{CB}^- plays an important role in the ET reaction rates and dynamics of photoexcited hydrated electrons in RM water pools.

Acknowledgment. We acknowledge support of this research by the Basic Energy Sciences Program of the Department of Energy and the Robert A. Welch Foundation. We are grateful to Dr. Sung-Ju Moon for synthesis of SDSS.

References and Notes

(1) *Structure and Reactivity in Reverse Micelles*; Pileni, M. P., Ed.; Elsevier: Amsterdam, 1989.

(2) Calvo-Perez, V.; Beddard, G. S.; Fendler, J. H. *J. Phys. Chem.* **1981**, *85*, 2316.

(3) Pileni, M. P.; Hickel, B.; Ferradini, C.; Pucheault, J. *Chem. Phys. Lett.* **1982**, *92*, 308.

(4) Gebicki, J. L.; Bednarek, P. *J. Mol. Struct.* **2000**, *555*, 227.

(5) Laria, D.; Kapral, R. *J. Chem. Phys.* **2002**, *117*, 7712.

(6) Pileni, M. P.; Zemb, T.; Petit, C. *Chem. Phys. Lett.* **1985**, *118*, 414.

(7) Kotlarchyk, M.; Stephens, R. B.; Huang, J. S. *J. Phys. Chem.* **1988**, *92*, 1533.

(8) Hirai, M.; Kawai-Hirai, R.; Takizawa, T.; Yabuki, S.; Nakamura, K.; Hirai, T.; Kobayashi, K.; Amemiya, Y.; Oya, M. *J. Phys. Chem.* **1995**, *99*, 6652.

(9) Koper, G. J. M.; Sager, W. F. C.; Smeets, J.; Bedeaux, D. *J. Phys. Chem.* **1995**, *99*, 13291.

(10) Wines, T. H.; Dukhin, A. S.; Somasundaran, P. *J. Colloid Interface Sci.* **1999**, *216*, 303.

(11) Svergun, D. I.; Konarev, P. V.; Volkov, V. V.; Koch, M. H. J.; Sager, W. F. C.; Smeets, J.; Blokhuis, E. M. *J. Chem. Phys.* **2000**, *113*, 1651.

(12) Gauduel, Y.; Pommeret, S.; Yamada, N.; Migus, A.; Antonetti, A. *J. Am. Chem. Soc.* **1989**, *111*, 4974.

(13) Gebicki, J. L.; Gebicka, L.; Kroh, J. *J. Chem. Soc., Faraday Trans.* **1994**, *90*, 3411.

(14) Wong, M.; Graetzel, M.; Thomas, J. K. *Chem. Phys. Lett.* **1975**, *30*, 329.

(15) Bakale, G.; Beck, G.; Thomas, J. K. *J. Phys. Chem.* **1992**, *96*, 2328.

(16) Prezhdo, O. V.; Rossky, P. J. *J. Phys. Chem.* **1996**, *100*, 17094.

(17) Schnitker, J.; Motakabbir, K.; Rossky, P. J.; Friesner, R. *Phys. Rev. Lett.* **1988**, *90*, 456.

(18) Kee, T. W.; Lee, Y. J.; Barbara, P. F. To be submitted for publication.

(19) Kee, T. W.; Son, D. H.; Kambhampati, P.; Barbara, P. F. *J. Phys. Chem. A* **2001**, *105*, 8434.

(20) Yokoyama, K.; Silva, C.; Son, D. H.; Walhout, P. K.; Barbara, P. F. *J. Phys. Chem. A* **1998**, *102*, 6957.

(21) Keszei, E.; Nagy, S.; Murphrey, T. H.; Rossky, P. J. *J. Chem. Phys.* **1993**, *99*, 2004.

(22) Son, D. H.; Kambhampati, P.; Kee, T. W.; Barbara, P. F. *Chem. Phys. Lett.* **2001**, *342*, 571.

(23) Srilakshmi, G. V.; Chaudhuri, A. *Chem. Eur. J.* **2000**, *6*, 2847.

(24) Tamamushi, B.; Watanabe, N. *Colloid Polym. Sci.* **1980**, *258*, 174.

(25) Alexandridis, P.; Holzwarth, J. F.; Hatton, T. A. *J. Phys. Chem.* **1995**, *99*, 8222.

(26) Tauber, M. J.; Mathies, R. A. *J. Phys. Chem. A* **2001**, *105*, 10952.

(27) Casanovas, J.; Grob, R.; Delacroix, D.; Guelfucci, J. P.; Blanc, D. *J. Chem. Phys.* **1981**, *75*, 4661.

(28) This is consistent with the report that the absorption coefficient of solvated electrons in *n*-hexane (Baxendale, J. H.; Bell, C.; Wardman, P. *J. Chem. Soc., Faraday Trans. 1* **1973**, *69*, 776), a solvent similar to isooctane, is three times smaller than the absorption coefficient of e_{aq}^-, both at 650 nm (Hart, E. J.; Anbar, M. *The Hydrated Electron*; Wiley-Interscience: New York, 1970).

(29) Lee, Y. J.; Zhang, T.; Barbara, P. F. To be submitted for publication.

(30) Barbara, P. F.; Meyer, T. J.; Ratner, M. A. *J. Phys. Chem.* **1996**, *100*, 13148.

(31) As seen in eq 3, the yield of depletion is a function of position of an electron. In the analysis, three different cases were used to distribute the electron: (i) at the center of the RM ($r_e = 0$), (ii) at the close position to the interface keeping a distance of the minimum size of e_{aq}^- ($r_e = R_w - R_s$) where R_s is the radius of e_{aq}^- (∼3), and (iii) equally within a sphere of a radius of $r_e < R_w - R_s$. In case (iii), the potential energy difference is less than k_BT in a sphere and the electron is found with equal probability within the sphere. For all three cases of initial location of e_{aq}^-, the predicted ET yield of actual depletion increases with R_w (the dotted line in Figure 4b), which is opposite to the trend of the measured Y_D.